Journal of Physics Research and Education, Volume 3, March 2026

Density Functional Study of Nitric Oxide Adsorption on the Monoclinic WO_3 (001) Surface

Md Abu Sayeed Sujan and Suman Chatterjee*
Department of Physics, University of North Bengal, Siliguri, West Bengal, India

Tungsten oxide (WO_3) is an important n-type semiconductor widely used in resistive gas sensing applications. Understanding the microscopic mechanism governing gas adsorption and the resulting modification of electronic properties is essential for improving sensor performance. In this work, density functional theory calculations based on the full potential linearized augmented plane wave (FP-LAPW) method are implemented to investigate nitric oxide adsorption on the monoclinic WO_3 (001) surface. Structural optimization and electronic structure calculations are carried out using the generalized gradient approximation in the Perdew-Burke-Ernzerhof form, the modified Becke-Johnson potential and the Hubbard $+U$ correction. A $(2 \times 2 \times 1)$-slab model with a vacuum thickness of 15 $\mathring{A}$ is constructed to simulate the surface. The results show that nitric oxide (NO) adsorption modifies the electronic structure of WO_3 and reduces the band gap due to enhanced hybridization between the W-$5d$ and the O-$2p$ states. Among the considered adsorption configurations, adsorption at the tungsten top site in a bent geometry is found to be energetically most favorable with an adsorption energy of approximately -1.42 eV. The electronic redistribution induced by adsorption leads to increased conductivity, providing a microscopic explanation for NO sensing in WO_3 based gas sensors.

I. INTRODUCTION

Semiconducting metal oxides have long been regarded as an important class of materials for gas sensing applications because of their chemical stability, low cost and strong sensitivity to environmental gases [1]. Among these materials, tungsten trioxide (WO_3) has received considerable attention as an effective material for resistive gas sensors. WO_3 is an n-type semiconductor with a wide band gap and exhibits strong surface reactivity toward oxidizing and reducing gases [2]. These characteristics have enabled its application in detecting environmentally and technologically important species such as nitrogen oxides, hydrogen, ozone and volatile organic compounds. Nitric oxide (NO) is an important gas from environmental and biomedical perspectives [3]. Nitric oxide, a byproduct of combustion, significantly contributes to atmospheric pollution and the development of photochemical smog. Furthermore, exposure to high levels of nitric oxide can present considerable health hazards, thereby establishing the reliable detection of this gas as a critical technological goal [4]. Metal oxide semiconductor sensors, particularly those utilizing WO_3, have shown considerable sensitivity to nitric oxide, a characteristic attributed to the strong interaction between tungsten surface sites and nitrogen-oxygen molecules [5]. The sensing mechanism in resistive metal oxide gas sensors is primarily dictated by surface adsorption processes

* suman@nbu.ac.in

[6]. Specifically, when gas molecules interact with the semiconductor surface, charge transfer occurs between the gas molecules and the solid surface. The alteration of electronic structure at the surface, resulting from this interaction, modifies the concentration of free charge carriers. This phenomenon influences electrical conductivity. While experimental techniques yield valuable insights into sensing performance, they frequently lack the capacity to directly visualize the atomic-scale processes governing adsorption and charge transfer. First-principles electronic structure calculations, grounded in density functional theory (DFT), present a complementary approach for investigating these phenomena. DFT calculations facilitate the accurate prediction of adsorption energies, electronic band structures and density of states, thus enabling a comprehensive understanding of gas sensing processes.

Among the available computational methods, the full potential linearized augmented plane wave (FP-LAPW) method is considered one of the most accurate implementations of density functional theory for crystalline solids [7]. This method treats the potential and charge density without shape approximations and is implemented in the WIEN2k software package, which has been widely applied to investigate the electronic structure of complex materials. In this work, nitric oxide adsorption on the monoclinic WO_3 (001) surface is investigated using density functional theory within the FP-LAPW formalism implemented in the WIEN2k code [8]. The structural and electronic properties of pristine WO_3 are examined using several exchange-correlation approximations, including GGA-PBE, the modified Becke-Johnson potential and the Hubbard $+U$ correction [9]. A surface slab model of the WO_3 (001) surface is created, and various adsorption configurations of the NO molecule are examined. To elucidate the impact of nitric oxide adsorption on the electronic structure of WO_3 and its influence on the conductivity, adsorption energies, band structures and density of states are analyzed. This analysis offers insights into the sensing characteristics of WO_3-based nitric oxide gas sensors.

II. COMPUTATIONAL METHODOLOGY

The exchange–correlation effects were treated using the generalized gradient approximation in the Perdew–Burke–Ernzerhof (PBE) [10] form for structural optimization. Since conventional GGA functionals are known to underestimate band gaps in semiconductors, additional calculations were performed using the modified Becke–Johnson (mBJ) [11] exchange potential to obtain improved band gap predictions. Furthermore, the Hubbard $+U$ [12] correction was introduced to account for the on-site Coulomb interaction among localized tungsten $5d$ electrons. The inclusion of the $+U$ term improves the description of electronic localization and orbital hybridization effects that are important for transition metal oxides. These complementary exchange–correlation treatments enable a comprehensive assessment of the electronic structure of WO_3 and allow evaluation of the sensitivity of adsorption-induced electronic changes to the chosen functional.

The electronic structure calculations were carried out using the WIEN2k implementation of the full potential linearized augmented plane wave (FP-LAPW) method. The muffin–tin radii (R_{MT}) were chosen as 1.90 bohr for W and 1.60 bohr for O atoms. The plane wave cutoff was controlled by the parameter RK_{max}, defined as the product of the smallest muffin–tin radius and the maximum reciprocal lattice vector and was set to $RK_{max} = 7.0$. The Brillouin zone integrations were performed using a Monkhorst–Pack k-point mesh of $8 \times 8 \times 8$ for bulk calculations. For the surface slab calculations a reduced k-point grid of $6 \times 6 \times 1$ was used due to the enlarged supercell along the surface normal direction. The self-consistent field iterations were continued until the total energy convergence criterion of 10^{-5} Ry was achieved. Structural relaxations were

performed until the residual forces acting on each atom were less than 1 mRy/bohr. To simulate the WO_3 (001) surface, a slab model constructed from a $2 \times 2 \times 1$ supercell was employed. The slab consisted of several atomic layers separated by a vacuum region of $15\mathring{A}$ along the surface normal direction in order to avoid spurious interactions between periodic images. During structural relaxation the atomic positions of the surface layers were allowed to relax while maintaining the periodic boundary conditions of the slab model. The separation between core and valence states was set to -6.0 Ry. All calculations were performed within the scalar relativistic approximation, which is appropriate for the electronic structure of tungsten oxides.

III. STRUCTURAL MODELING OF WO_3

Tungsten oxide crystallizes in several polymorphic phases depending on temperature and pressure [13]. Among these phases, the monoclinic structure is the thermodynamically stable form at room temperature and is therefore the most commonly investigated phase for gas sensing applications [14]. The monoclinic phase exhibits significant distortion of the WO_6 octahedral framework, which strongly influences its electronic structure and surface reactivity. The bulk structure of WO_3 was constructed using experimentally reported crystallographic parameters obtained from the Materials Project database. The crystal belongs to the monoclinic system with space group $P2_1/c$. In this structure, tungsten atoms occupy the centers of distorted WO_6 octahedra formed by six surrounding oxygen atoms. These octahedra are connected through corner-sharing oxygen atoms, producing a three-dimensional network characteristic of many transition metal oxides. The lattice parameters used to construct the initial structure are summarized in Table I. These parameters serve as the starting point for the electronic structure calculations.

TABLE I: Lattice parameters of monoclinic WO_3 used for structural modeling.

$a(\mathring{A})$	$b(\mathring{A})$	$c(\mathring{A})$	α (°)	β (°)	γ (°)	Volume $(\mathring{A}^3)$
5.359	5.415	7.725	89.086	90	90	224.132

The crystal structure was visualized and manipulated using the VESTA software package. The bulk unit cell obtained from crystallographic data was first examined to verify atomic positions and bonding environments. Particular attention was given to the coordination geometry of tungsten atoms and the arrangement of oxygen atoms forming the distorted octahedral framework. Figure 1 illustrates the crystal structure of monoclinic WO_3. Tungsten atoms are located at the centers of WO_6 octahedra, while oxygen atoms occupy the vertices of the octahedral units. The distortion of these octahedra leads to variations in W–O bond lengths and bond angles, which play an important role in determining the electronic properties of the material.

A. Surface slab model

To investigate nitric oxide adsorption, the WO_3 (001) surface was modeled using a periodic slab geometry constructed from the optimized monoclinic WO_3 bulk structure. A $2 \times 2 \times 1$ surface supercell was generated in order to provide sufficient lateral separation between periodic images of the adsorbed molecule and to reduce artificial interactions caused by periodic boundary conditions. The resulting slab model contains 64 atoms consisting of 16 W atoms and 48 O

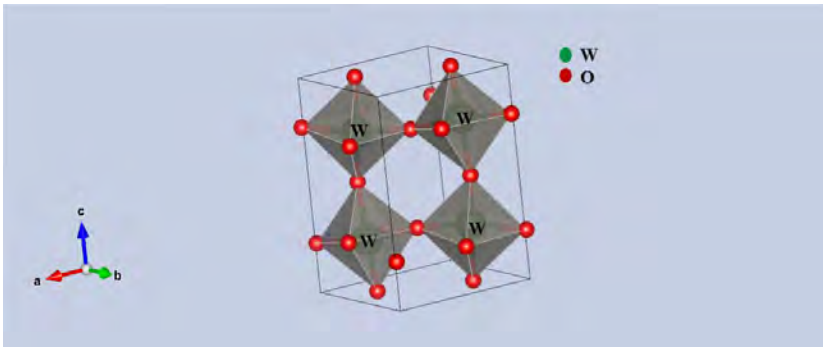

FIG. 1: Crystal structure of monoclinic WO_3

atoms. A vacuum layer of 15 $\mathring{A}$ was introduced along the surface normal direction to eliminate spurious interactions between periodically repeated slabs. No symmetry constraints were applied in the surface calculations so that the adsorption system could relax without artificial restrictions. During structural relaxation, the atoms in the upper surface layers together with the adsorbed nitric oxide molecule were allowed to relax fully until the force convergence criterion was satisfied. The atoms in the bottom layer of the slab were kept fixed at their bulk positions in order to mimic the bulk environment beneath the surface. For the adsorption calculations, a single NO molecule was placed on the WO_3 (001) surface within the $2 \times 2 \times 1$ supercell. This corresponds to a low surface coverage that minimizes interactions between neighboring adsorbate molecules. Several initial adsorption configurations were examined, including the tungsten top site, oxygen bridge site and hollow site, and the system was fully relaxed to determine the most stable adsorption geometry. The constructed WO_3 (001) surface slab together with the vacuum region used in the calculations is shown in Fig. 2.

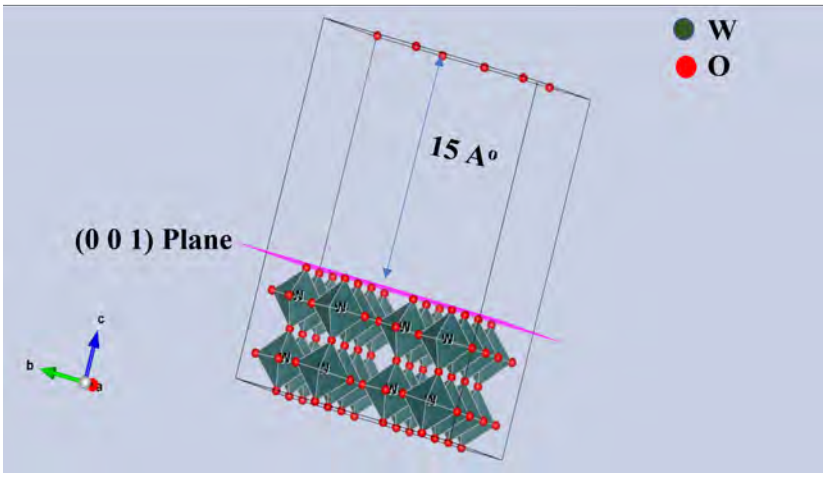

FIG. 2: Surface slab model of the WO_3 (001) surface constructed using a $2 \times 2 \times 1$ supercell with a vacuum region of 15$\mathring{A}$ along the surface normal direction.

IV. ELECTRONIC PROPERTIES OF PRISTINE WO_3

The electronic structure of pristine monoclinic WO_3 was investigated through band structure and density of states calculations using several exchange–correlation approximations [15]. The electronic structure of the pristine material is essential before analyzing the influence of gas adsorption, since adsorption-induced sensing behavior originates from modifications of the host electronic states near the Fermi level.

A. Band structure

The electronic band structure of pristine monoclinic WO_3 was calculated along the high–symmetry directions of the Brillouin zone in order to analyze the distribution of electronic states near the Fermi level. The band structure provides a direct view of the allowed energy levels of electrons, depending on their crystal momentum. This determines the basic electronic and transport properties of the material [16]. The calculated electronic band structures obtained using the PBE, modified Becke–Johnson (mBJ) and DFT+U exchange–correlation approaches are presented in Fig. 3. In PBE and DFT+U it shows indirect band gap when we used modified Becke-Johnson (mBJ) WO_3 exhibits semiconducting behavior with a direct band gap. Within the PBE approximation the calculated band gap is approximately 0.82 eV. This small value reflects the well known tendency of standard generalized gradient approximation functionals to underestimate the band gaps of semiconductors and transition metal oxides. This underestimation is due to limitations in how exchange interactions are described [17]. A more accurate description of the electronic structure is obtained when the modified Becke–Johnson exchange potential is employed. The mBJ calculation increases the band gap to approximately 2.0 eV, representing an improvement compared with the PBE result and brings the predicted value closer to experimentally reported band gaps for monoclinic WO_3. Further improvement is observed when the Hubbard $+U$ correction is introduced to account for the on-site Coulomb interaction among the localized tungsten $5d$ electrons. The DFT+U calculation yields a band gap of approximately 2.6–2.7 eV. The incorporation of the Hubbard correction facilitates the localization of tungsten $5d$ orbitals, thereby widening the gap between valence and conduction bands; this leads to a more accurate depiction of the electronic structure. These findings underscore the significant impact of the selected exchange–correlation functional on the electronic characteristics of WO_3, and they emphasize the necessity of refined exchange treatments in the investigation of transition metal oxides. The subsequent calculations were done using this DFT+U approach.

The use of these complementary exchange–correlation approaches allows a systematic comparison of the predicted electronic structure. In particular, the PBE functional provides a baseline description of the system, the mBJ potential improves the prediction of band gaps, and the DFT+U method accounts for the strong Coulomb interaction associated with the tungsten $5d$ states. The calculated band gaps obtained using different exchange–correlation treatments for pristine WO_3 are summarized in Table II. The results clearly illustrate the well-known band gap underestimation within conventional GGA and the improved description obtained using mBJ and DFT+U approaches. These approaches enable a comprehensive assessment of how the choice of exchange–correlation functional influences the electronic structure of WO_3 and provide a reliable foundation for analyzing adsorption-induced electronic modifications on the WO_3 (001) surface.

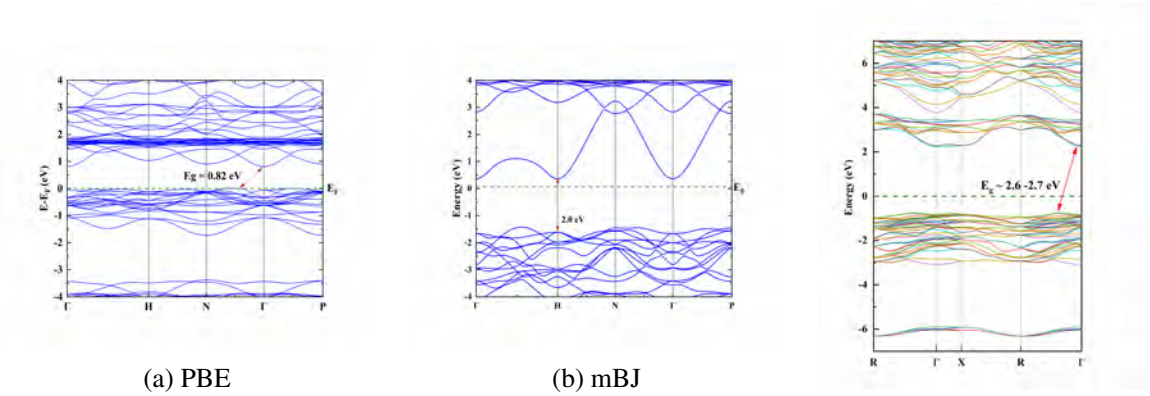

(a) PBE (b) mBJ (c) DFT+U

FIG. 3: Band structures of pure monoclinic WO_3 using three exchange–correlation approaches: (a) PBE, (b) modified Becke–Johnson (mBJ) and (c) DFT+U. The Fermi level is set to 0 eV.

TABLE II: Comparison of exchange–correlation treatments used in the present calculations and the corresponding band gaps obtained for monoclinic WO_3.

Functional	Type	Exchange Treatment	Correlation Treatment	Band Gap (eV)
GGA–PBE	GGA	Gradient corrected exchange	Gradient corrected correlation	0.82
mBJ–LSDA	Semi-local potential	Modified BJ exchange potential	Local spin density correlation	2.0
DFT+U	Hubbard corrected DFT	GGA exchange with on-site Coulomb correction	GGA correlation with Hubbard $+U$ term	2.6

B. Density of states

To obtain deeper insight into the electronic structure of monoclinic WO_3, the total and atom-resolved density of states (DOS) were calculated using three different exchange–correlation approaches: the PBE functional, the modified Becke–Johnson (mBJ) potential and the DFT+U method. The density of states provides information about the distribution of electronic states as a function of energy and allows identification of the contributions from different atomic species in the material. Figure 4 presents the calculated total density of states together with the contributions originating from tungsten and oxygen atoms for pristine WO_3. In all DOS plots the Fermi level is set to zero energy. The findings indicate that the electronic states within the valence band are predominantly influenced by oxygen atoms, whereas the conduction band is primarily constituted of tungsten-derived states. This distribution mirrors the electronic structure linked to the distorted WO_6 octahedral framework, which constitutes the crystal lattice of monoclinic WO_3. The density of states derived from the PBE functional exhibits a relatively narrow separation between the

valence and conduction bands, aligning with the underestimation of the band gap observed in the corresponding band structure calculations. When the modified Becke–Johnson potential is employed, a clearer separation between the occupied and unoccupied states is observed. The mBJ potential improves the description of the exchange potential and therefore produces a larger band gap compared with the PBE functional. As a result, the DOS calculated with mBJ shows a more pronounced separation between the valence band and the conduction band. Further modification of the electronic structure is observed when the Hubbard $+U$ correction is introduced. Including the on-site Coulomb interaction strengthens the localization of tungsten's electronic states, which then shifts the conduction band to higher energy levels. Consequently, the DFT+U calculations produce an even larger band gap and a more distinct separation between the occupied and unoccupied electronic states. These states are, in turn, critical determinants of the transport characteristics exhibited by WO_3. Understanding the distribution of these electronic states in the pristine material is particularly important for analyzing adsorption processes, since interactions between gas molecules and surface atoms can modify the electronic structure near the Fermi level. The DOS obtained for pristine WO_3 therefore provides an important reference for evaluating the changes in electronic structure that occur when nitric oxide molecules adsorb on the WO_3 surface.

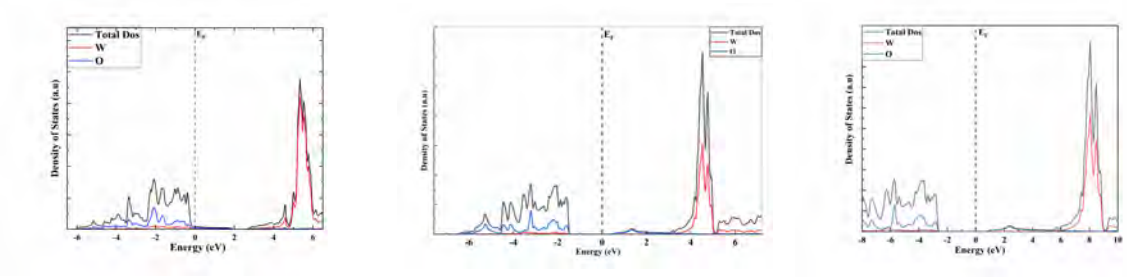

(a) PBE (b) mBJ (c) DFT+U

FIG. 4: Total and atom-resolved density of states of pristine monoclinic WO_3 calculated using three exchange–correlation approaches: (a) PBE, (b) modified Becke–Johnson (mBJ) and (c) DFT+U. The contributions from tungsten and oxygen atoms are shown separately. The Fermi level is set to 0 eV.

V. ADSORPTION GEOMETRY OF NITRIC OXIDE

The adsorption of nitric oxide molecules on the WO_3 (001) surface was investigated in order to understand the microscopic origin of the sensing response in WO_3 based gas sensors. Gas sensing in semiconducting metal oxides is primarily controlled by surface adsorption. This process involves gas molecules interacting with surface atoms, which causes a redistribution of electronic charge [18]. These interactions change the local electronic structure near the surface, affecting semiconductor's carrier concentration and, therefore, its electrical conductivity [19]. As a result, understanding how nitric oxide adsorbs on the WO_3 surface is essential for explaining the sensing mechanism of WO_3-based NO gas sensors. To determine the preferred adsorption geometry of the NO molecule on the WO_3 (001) surface, several possible adsorption configurations were systematically examined. The NO molecule was initially placed at three representative surface sites: the tungsten top site (W-top), the oxygen bridge site (O-bridge) and the hollow site formed

by surrounding surface atoms. These adsorption environments represent the most typical binding locations encountered on transition metal oxide surfaces. For each configuration the NO molecule was placed at an appropriate initial distance above the surface and the entire system was allowed to relax so that both the adsorbate and the nearby surface atoms could adjust their positions freely until the total energy of the system reached its minimum value. This structural adjustment ensures that the final adsorption geometries correspond to stable equilibrium states. The considered adsorption sites are illustrated schematically in Fig. 5.

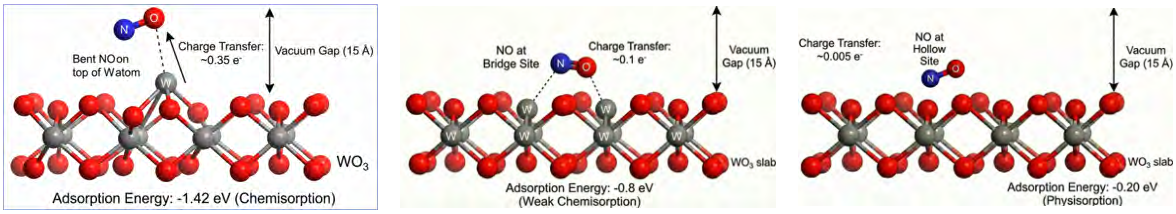

(a) W-top (tilted) (b) O-bridge (c) Hollow site

FIG. 5: Adsorption configurations of the NO molecule on the WO_3 (001) surface: (a) adsorption at the tungsten top site with a tilted geometry, (b) adsorption at the oxygen bridge site and (c) adsorption at the hollow site.

The relative stability of the different adsorption configurations was evaluated by calculating the adsorption energy. Adsorption energy, defined by

$$E_{ads} = E_{\mathrm{NO/WO_3}} - (E_{\mathrm{WO_3}} + E_{\mathrm{NO}}) \,, \tag{1}$$

provides a quantitative measure of the interaction strength between the adsorbed molecule and the surface. In the above equation, $E_{\mathrm{NO/WO_3}}$ signifies the total energy of the WO_3 surface with the adsorbed NO molecule, $E_{\mathrm{WO_3}}$ represents the energy of the pure WO_3 surface and E_{NO} corresponds to the energy of an isolated nitric oxide molecule. A negative adsorption energy value suggests that the adsorption process is energetically favorable; conversely, larger negative values indicate a stronger interaction between the adsorbate and the surface [20]. The calculated adsorption energies together with the corresponding interaction characteristics are summarized in Table III. The

TABLE III: Adsorption configurations and the corresponding energies of NO on the WO_3 (001) surface.

Adsorption Site	Adsorption Energy (eV)	Interaction Type	Geometry Description
W-top (tilted)	-1.42	Strong chemisorption	NO molecule tilted toward the surface tungsten atom
O-bridge	-0.50 to -0.80	Weak chemisorption	NO positioned between two neighboring surface oxygen atoms
Hollow site	-0.10 to -0.30	Physisorption	Weak interaction with surrounding surface atoms without direct bonding

results show that the tungsten top site is the most energetically favorable configuration for adsorption, with an adsorption energy of about -1.42 eV. After structural relaxation the NO molecule adopts a tilted orientation relative to the surface plane, with the nitrogen atom directed toward the surface tungsten atom. The bent configuration indicates strong chemical interaction between the molecular orbitals of nitric oxide and the tungsten $5d$ orbitals of the surface atom. Adsorption at the oxygen bridge site exhibits weaker interaction with adsorption energies between -0.50 eV and -0.80 eV, indicating weak chemisorption. In this geometry the molecule interacts simultaneously with two neighboring oxygen atoms, resulting in a less favorable bonding environment compared with the tungsten top site. The hollow site configuration represents the least stable adsorption geometry, with adsorption energies between -0.10 eV and -0.30 eV, which indicates very weak interaction dominated primarily by van der Waals forces and therefore corresponds to physisorption. The strong stability of the tungsten top configuration can be explained by considering the electronic structure of WO_3. Surface tungsten atoms possess partially filled $5d$ orbitals that can interact efficiently with the molecular orbitals of nitric oxide. This interaction enhances orbital hybridization and leads to charge redistribution at the adsorption site, which modifies the electronic structure near the Fermi level [21]. Such adsorption-induced electronic changes influence the conductivity of the material and play an important role in the sensing mechanism of WO_3 based nitric oxide gas sensors.

VI. ELECTRONIC STRUCTURE OF WO_3 AFTER ADSORPTION OF NO MOLECULES

To understand how the electronic properties of the WO_3 surface change when nitric oxide is adsorbed, we calculated the electronic band structure and density of states. This was done for the optimized adsorption configuration of the NO molecule on the WO_3 (001) surface. When gas molecules adsorb onto semiconductor surfaces, the electronic structure changes. This happens because of charge redistribution and the interaction between the adsorbate's electronic states and those of the substrate. These interactions can create new electronic states near the band edges and change the distribution of electronic states around the Fermi level. These adsorption-induced electronic changes are particularly important for semiconducting metal oxide gas sensors. The sensing mechanism in these sensors is directly related to changes in electrical conductivity caused by surface interactions [22]. The calculated electronic band structure of the NO adsorbed WO_3 (001) surface is presented in Fig. 6. The band dispersion reveals that the overall semiconducting nature of the material is preserved after adsorption; however, significant modifications occur in the vicinity of the band edges. In particular, the band gap of the adsorption system becomes noticeably smaller compared with that of pristine WO_3. The pristine system, as determined by the DFT+U method, displays a band gap of roughly 2.6 eV. Conversely, the band gap of the adsorption system diminishes to approximately 1.8 eV following the adsorption of the NO molecule. This observed band gap reduction suggests that the interaction between the nitric oxide molecule and the WO_3 surface introduces supplementary electronic states, thereby affecting the energy difference between the valence band maximum and the conduction band minimum.

The observed band gap reduction originates from the interaction between the molecular orbitals of nitric oxide and the surface states of WO_3. The presence of the adsorbed molecule perturbs the electronic potential near the surface and modifies the dispersion of the electronic bands. As a consequence, new electronic states appear in the vicinity of the band edges, effectively reducing the energy separation between the valence and conduction bands. The narrowing of the band gap indicates that the adsorption process alters the electronic transport characteristics of the surface

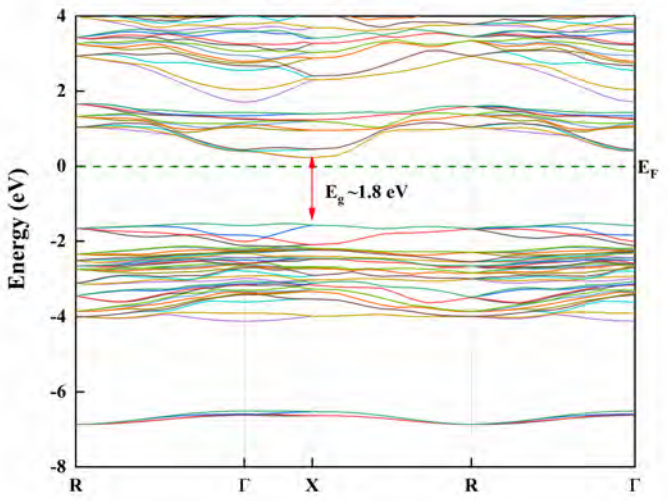

FIG. 6: Electronic band structure of the NO adsorbed WO_3 (001) surface calculated using the DFT+U approach. The adsorption of nitric oxide leads to a reduction of the band gap to approximately 1.8 eV. The Fermi level is set to 0 eV.

region. Further insight into the adsorption-induced electronic modifications can be obtained from the analysis of the density of states. The calculated total and atom-resolved density of states for the NO adsorbed WO_3 surface are shown in Fig. 7. In addition to the contributions from tungsten and oxygen atoms forming the WO_3 lattice, the DOS also contains contributions from the nitrogen atom belonging to the adsorbed NO molecule. This allows identification of the electronic states associated with the adsorbate and their interaction with the substrate.

The conduction band region continues to be mainly composed of tungsten-derived states associated with the electronic states of the surface tungsten atoms. However, after adsorption of nitric oxide, additional electronic states appear close to the Fermi level. These states originate from the electronic states of the adsorbed NO molecule and from the interaction between the adsorbate and the surface tungsten atom. The presence of nitrogen-derived states in the density of states confirms that the adsorbed molecule contributes directly to the electronic structure of the surface system. These nitrogen-related states interact with the electronic states of the substrate, producing hybridized electronic states that extend across the adsorbate–substrate interface. Such hybridization is a signature of chemical interaction between the nitric oxide molecule and the WO_3 surface. The interaction modifies the distribution of electronic states near the Fermi level and leads to the formation of additional electronic states within the band structure. The appearance of these additional states near the Fermi level contributes to the narrowing of the band gap observed in the band structure. Because the band gap determines the energy required for electronic excitation, its reduction implies that charge carriers can be generated more easily in the adsorption system. Consequently, the number of available electronic states participating in electrical conduction increases. This increase in the availability of charge carriers can lead to an enhancement of the electrical conductivity of the WO_3 surface after adsorption of nitric oxide molecules. From the perspective of gas sensing applications, this adsorption-induced modification of the electronic structure plays a

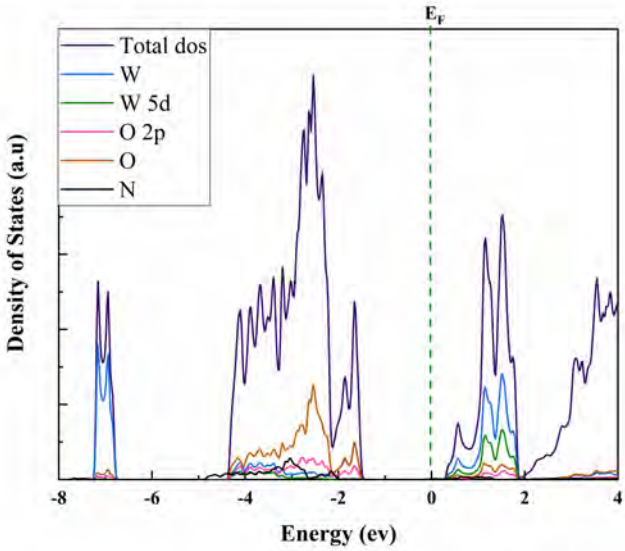

FIG. 7: Total and atom-resolved density of states of the NO adsorbed WO_3 (001) surface calculated using the DFT+U method. Contributions from tungsten (W), oxygen (O) and nitrogen (N) atoms are shown. The Fermi level is set to 0 eV.

critical role in determining the sensing behavior of WO_3 based gas sensors. When NO molecules adsorb on the WO_3 surface, the resulting charge redistribution and orbital interaction modify the electronic states of the material and reduce the band gap. The increased density of states near the Fermi level facilitates charge transport and modifies the electrical resistance of the sensor material. The change in electrical conductivity arising from these electronic structure modifications forms the fundamental mechanism underlying the sensing response of WO_3 based nitric oxide gas sensors.

VII. CONCLUSION

In this work a first-principles investigation of nitric oxide adsorption on the monoclinic surface of WO_3 (001) was carried out using functional density theory within the full potential linearized augmented plane wave framework implemented in the WIEN2k code. The structural and electronic properties of the pristine WO_3 were first examined using several exchange–correlation approaches, including the modified Becke–Johnson potential, GGA–PBE and the Hubbard $+U$ correction, in order to obtain a reliable description of the electronic structure of the material. The calculated electronic band structures confirm that monoclinic WO_3 behaves as a semiconductor with a band gap that depends strongly on the exchange–correlation treatment. The GGA–PBE functional yields a smaller band gap due to the well-known underestimation of exchange effects, whereas the mBJ and DFT+U approaches provide improved descriptions of the electronic structure by accounting for exchange enhancement and on-site Coulomb interactions associated with tungsten $5d$ electrons. The adsorption behavior of nitric oxide on the WO_3 (001) surface was

systematically investigated by examining several possible adsorption configurations. Among the considered adsorption sites, the tungsten top site was found to be the most energetically favorable with an adsorption energy of approximately -1.42 eV. The NO molecule adopts a tilted configuration in this geometry, indicating strong chemical interaction between the adsorbate and the surface tungsten atoms. Adsorption at the oxygen bridge site exhibits weaker interaction corresponding to weak chemisorption, while the hollow site shows very small adsorption energies characteristic of physisorption. Electronic structure analysis reveals that adsorption of nitric oxide significantly modifies the electronic properties of the WO_3 surface. The band gap of the system decreases after adsorption, indicating the introduction of additional electronic states near the band edges. Density of states analysis further shows enhanced hybridization between tungsten $5d$ and oxygen $2p$ orbitals near the Fermi level, which reflects strong interaction between the adsorbed molecule and the substrate. These adsorption-induced electronic modifications are expected to influence the electrical conductivity of the material and provide an insight into the sensing mechanism of WO_3 based nitric oxide gas sensors. The present study demonstrates how first-principles calculations can provide detailed insight into the relationship between surface chemistry and electronic properties in gas sensing materials, thereby contributing to the design of more efficient semiconductor gas sensors.

Acknowledgments : The authors are grateful to the Department of Physics, NBU and Prof. Pradip Kumar Mandal for providing the computational facilities required for this research work.

[1] N. A. Isaac, I. Pikaar and G. Biskos, Mikrochimica Acta **5**, 189 (2022).
[2] C. Dong, R. Zhao, L. Yao, Y. Ran, X. Zhang and Y. Wang, J. Alloy. Compd. **820**, 153194 (2020).
[3] J. Wang *et al.,* Sensors and Actuators B **417**, 136157 (2024).
[4] I. Manisalidis, E. Stavropoulou, A. Stavropoulos and E. Bezirtzoglou, Front. Pub. Health **8**, 14 (2020).
[5] R. Nagpal, N. Ababii and O. Lupan, Mat. Today Elec. **15**, 100192 (2026).
[6] A. Staerz, U. Weimar and N. Barsan, Sensors **16**, 10 (2016).
[7] O. Castro-Ocampo *et al.*, Theor. Comp. Chem. **25**, 391 (2025).
[8] M. Petersen, F. Wagner *et al.*, Comp. Phys. Commun. **126**, 294 (2000).
[9] S. Landron and M. B. Lepetit, Phys. Rev. B **77**, 3 (2008).
[10] J. P. Perdew, K. Burke and M. Ernzerhof, Phys. Rev. Lett. **77**, 3865 (1996).
[11] J. A. Camargo-Martinez and R. Baquero, Phys. Rev. B **86**, 195106 (2012).
[12] B. Himmetoglu, A. Floris, S. de Gironcoli and M. Cococcioni, Int. J. Quant. Chem. **114**, 14 (2014).
[13] E. Cazzanelli, C. Vinegoni, G. Mariotto, A. Kuzmin and J. Purans, J. Solid State Chem. **143**, (1999).
[14] S. Yang *et al.*, ACS Appl. Nano Mat. **5**, 16544 (2022).
[15] P. Borlido *et al.*, Comp. Mat. **6** (2020); *ibid.* **6**, 96 (2020).
[16] S. Bashir *et al.*, Heliyon **10**, 34553 (2024).
[17] S. Bhattacharjee, N. A. Koshi and S. C. Lee, Phys. Chem. Chem. Phys. **26**, 26443 (2024).
[18] G. Mineo, K. Moulaee, G. Neri, S. Mirabella and E. Bruno, Chemosensors **10**, 11 (2022).
[19] G. M. Moussounda Mba *et al.*, Surface and Interface Analysis **58**(5), 334 (2026).
[20] C Xiao *et al.,* ACS Omega **7**, 8706 (2022).
[21] J. Kröger, L. Limot, H. Jensen, R. Berndt, S. Crampin and E. Pehlke, Prog. Surf. Sci. **80**, 26 (2005).
[22] S. Sahare *et al.,* Adv. Opt. Mat. **13**, e01747 (2025).